PHILOSOPHICAL TRANSACTIONS OF THE ROYAL SOCIETY A
MATHEMATICAL, PHYSICAL & ENGINEERING SCIENCES

Optical in situ Surface Control during MOVPE and MBE Growth [and Discussion]

Wolfgang Richter and J. F. McGilp

Phil. Trans. R. Soc. Lond. A 1993 **344**, 453-467
doi: 10.1098/rsta.1993.0100

Optical *in situ* surface control during MOVPE and MBE growth

By Wolfgang Richter

Technische Universität Berlin, Institut für Festkörperphysik, Hardenberg Str. 36,
1000 Berlin 12, F.R.G.

Reflectance anisotropy spectroscopy (RAS) and Raman scattering are presented as *in situ* and online analytical tools for epitaxial growth of semiconductors. While RAS derives its surface sensitivity from an anisotropic surface structure, Raman scattering has monolayer resolution at heterointerfaces due to the fingerprint character of the vibrational properties of the overlayers. The growth examples discussed are MOVPE growth of GaAs on GaAs analysed by RAS and MBE growth of InSb on Sb as well as CdTe on InSb monitored by Raman scattering. The information gained concerns the status of the pregrowth surface (RAS), growth rate with monolayer resolution (RAS), growth morphology (Raman scattering) and the detection of interface reactions (Raman scattering). Both methods can be applied with a time resolution of a few seconds (Raman scattering) or better (RAS).

1. Introduction

Epitaxial growth is one of the prerequisites for the fabrication of semiconductor devices and multilayer structures. Out of the many epitaxial growth techniques which have been developed over the past decades two are nowadays most widely in use. One of them is the molecular beam epitaxy (MBE) where under ultrahigh vacuum (UHV) conditions molecular beams of the elements, usually generated from effusions cells, are utilized to deposit the desired material (Herman & Sitter 1989). The other technique is the metal organic vapour phase epitaxy (MOVPE) which operates at pressures between 10 and 1000 mbar and uses metalorganic compounds of the elements to be deposited (Razeghi 1989). Both are thermal non-equilibrium methods. While in MBE, however, only surface reactions play a role, in MOVPE reactions in the gas phase as well as at surface are important. Both growth methods have been very successful in depositing thin layers down to a few monolayers (quantum wells) as well as thicker and complex multilayer structures. Preference to either of these both growth methods depends on the specific material to be grown but also on the laboratory environment (industrial or research).

As far as growth control is concerned, however, both methods are on a quite different level. While in the UHV environment of MBE all the by now 'classical' analytical methods of surface science can be applied, in MOVPE essentially no control instrument is available. For MBE the reflection high energy electron diffraction (RHEED) has developed as the standard *in situ* control technique. The appropriate RHEED pattern signals that the surface is now prepared to start growth and the intensity oscillations reveal the growth rate on the monolayer scale (Joyce 1985). As

Phil. Trans. R. Soc. Lond. A (1993) **344**, 453–467

Printed in Great Britain

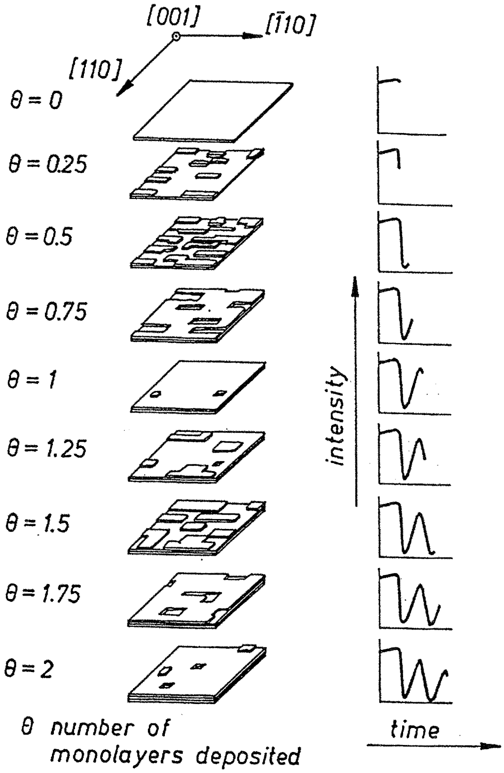

Figure 1. RHEED intensity oscillations originating from surface roughness at different GaAs monolayer coverages (after Joyce *et al.* 1986).

shown in figure 1 the intensity variations are caused by the difference in surface roughness between partly and fully completed layers. These oscillations disappear at continuous growth due to the increasing surface roughness, but usually can be re-established by growth interruptions. They disappear too at higher temperatures where the surface diffusion length has larger values and growth is dominantly appearing at surface steps (step flow growth) instead on the terraces in between.

In standard MOVPE, in contrast, no growth control is available and growth parameters are empirically established by correlating the flowmeter settings with sample properties determined by post growth analysis. Nevertheless, on the research level some progress has been made during the last ten years as far as the gas phase analysis is concerned and knowledge about the basic gas phase reaction steps of the metalorganic precursors has been considerably increased. This knowledge was to a large extent gained by relatively complex optical experiments and was used to speculate about possible surface reaction during growth. But no direct results from surface experiments were available.

In the presence of a gaseous ambient optical techniques of course in principle are the methods of choice in order to analyse semiconductor surfaces. Their surface sensitivity, nevertheless, is considered to be low because of the large penetration depth of the optical radiation (10–100 nm). However, in the last years progress has been made in the field of optical surface science techniques which have been termed also EPIOPTICS (McGilp 1990; Weightman 1991). Nonlinear methods like second harmonic generation (SHG) or linear techniques like surface photo absorption,

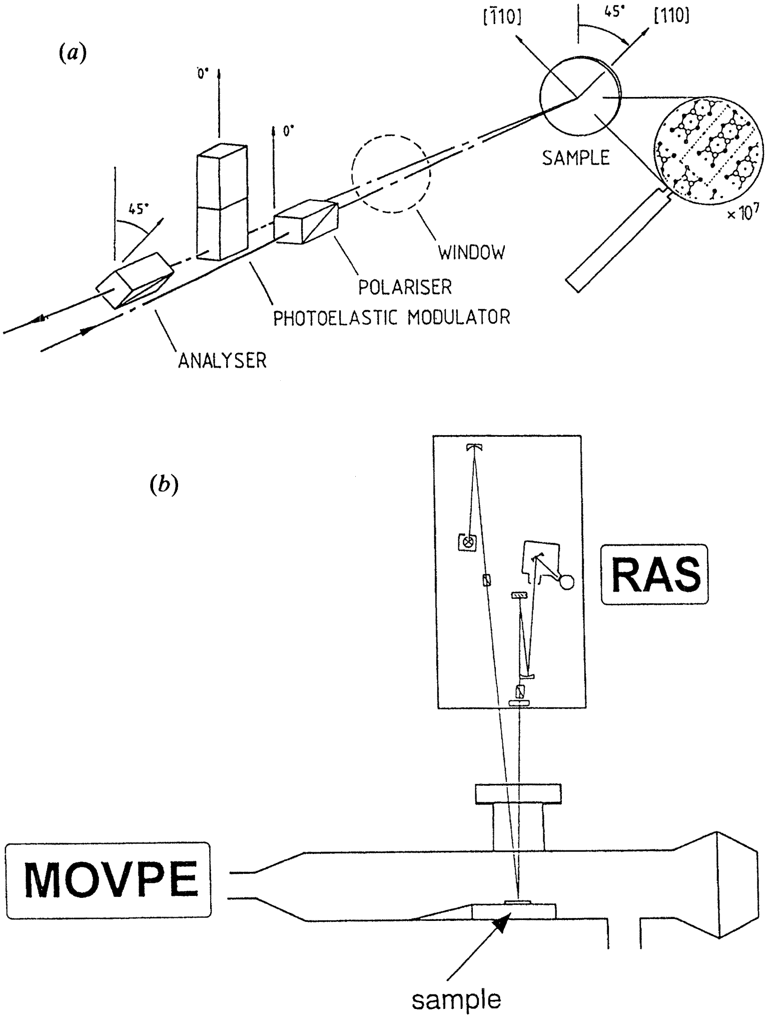

Figure 2. The reflectance anisotropy experiment: (*a*) schematic optical layout, (*b*) spectroscopic set up for monitoring MOVPE growth.

ellipsometry, Raman scattering and reflectance anisotropy spectroscopy have been pushed to a level where monolayer sensitivity is reached. It seems, therefore, feasible to use these optical techniques to control epitaxial growth or other surface modification processes. Although their introduction into *in situ* analysis is initiated by the need to characterize surfaces through a gas phase, especially in MOVPE, they may be as well applied in UHV, of course, to monitor MBE growth.

In this paper we will concentrate on reflections anisotropy spectroscopy (RAS) and Raman scattering. Raman scattering is applied to MBE growth of heterostructures and RAS to homoepitaxial growth of III–V-compounds. It will be shown that both optical techniques are powerful diagnostic techniques for the *in situ* and online analysis of epitaxial growth.

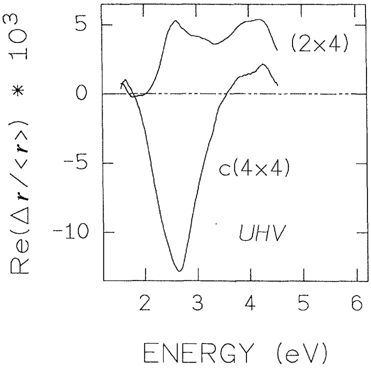

Figure 3. RAS spectra taken in an MBE set-up for GaAs (100) surfaces reconstructed (2×4) and $c(4\times 4)$ as determined by RHEED.

2. Reflection anisotropy spectroscopy during MOVPE

From its first basic demonstration (Aspnes 1985) reflectance anisotropy spectroscopy has shown to be a quite surface sensitive technique which was successfully applied in a number of growth studies (Aspnes *et al.* 1989; Koch *et al.* 1990; Samuelson *et al.* 1991; Scholz *et al.* 1992).

The schematic layout of a reflectance anisotropy measurement is shown in figure 2*a*. The photoelastic modulator introduces a phaseshift via the elastoopic effect to the linearly polarized light. By this the light polarization is alternating between the two directions in the surface, $[\bar{1}10]$ and $[110]$, and the corresponding reflectivities can be measured. The modulation frequency for this phaseshift is usually 50 kHz. If the reflectance for light polarized in the two directions is different, i.e. the surface is optically anisotropic, an AC component will occur in the reflected light signal. If the reflectivities are the same, the AC signal will be zero. This differential technique allows to determine values of $\Delta r/r$ in the range of 10^{-5}. The quantity measured usually is the real part of the normalized reflectance:

$$\mathrm{Re}\,\Delta r/r = \mathrm{Re}\,2(r_{\bar{1}10}-r_{110})/(r_{\bar{1}10}+r_{110}). \tag{1}$$

In cubic materials like diamond and zincblende type semiconductors the bulk possesses no anisotropic contribution to first order because these crystals are optically isotropic by symmetry. Thus anisotropic reflectivities can only originate from the surface with different symmetry. Such a case is sketched in figure 2*a* for a GaAs(100)–(2×4) surface where clearly the optical response is expected to be anisotropic. For MOVPE growth studies the RAS equipment can be easily fitted to the growth reactor. Figure 2*b* shows a spectroscopic RAS setup on top of a MOVPE reactor.

The first RAS measurements have been made in UHV (MBE) with well-defined reconstructions of GaAs(100) surfaces measure by RHEED (Aspnes *et al.* 1990) and later on by LEED (Resch *et al.* 1992). From these measurements it was possible to correlate certain reconstructions with certain RAS spectra. Figure 3 gives an example. The GaAs(100)–(2×4) shows up in the RAS spectra with a typical camel back like shape, while the GaAs(100)–$c(4\times 4)$ is characterized by a deep minimum at 2.6 eV. Tight binding calculations with an approximated surface structure indicate that the 2.6 eV structure is due to electronic transition from occupied lone pair bands into unoccupied As dimer bands (Chang 1990) and is therefore characteristic for As dimers. If the dimers redirect themselves when the surface reconstructs Δr will

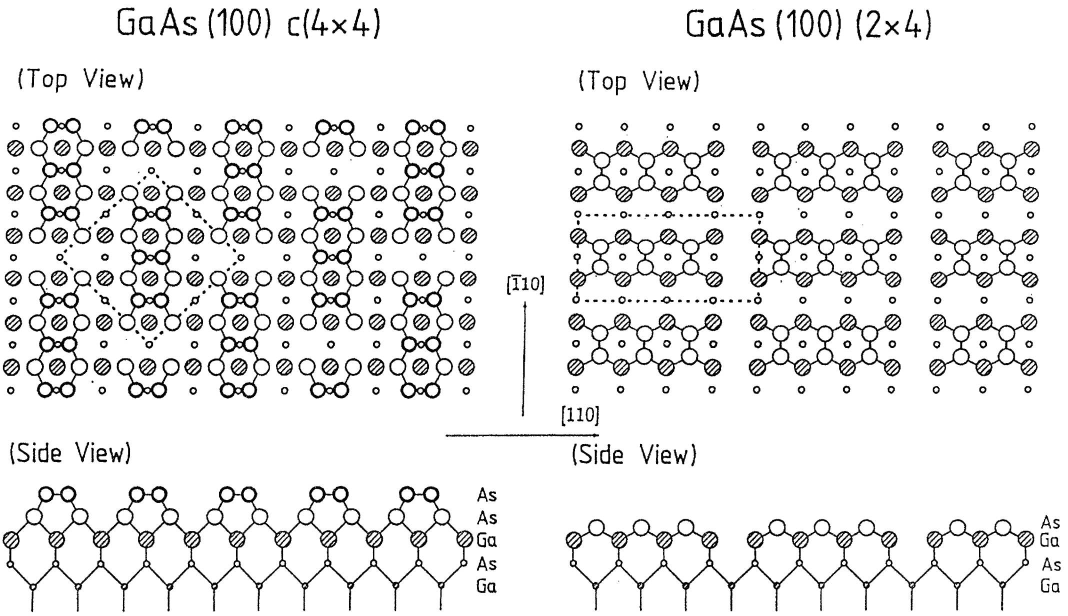

Figure 4. Surface structure of GaAs(100)–$c(4\times4)$ and GaAs(100)–(2×4) (after Biegelsen 1990).

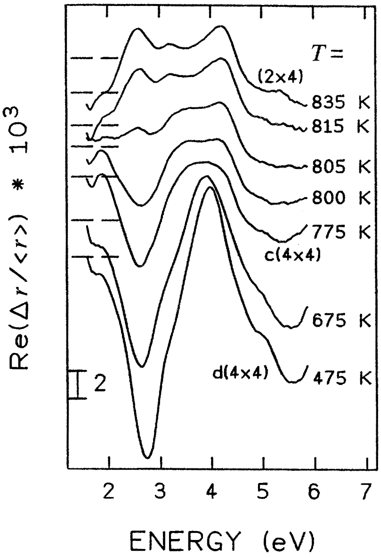

Figure 5. RAS spectra of GaAs(100) in an MOVPE reactor at different temperatures and $p(H_2) = 100$ mbar.

change, too. A change of sign in Δr is even expected according to (1) for the (2×4) and $c(4\times4)$ surfaces as shown in figure 4. For the (2×4) the dimers are along $[\bar{1}10]$ and for the $c(4\times4)$ along [110]. Figure 3 indeed shows that Δr changes sign.

Identical RAS spectra have been reported under hydrogen ambient (Kamiya *et al.* 1992). Figure 5 gives a similar example taken in a MOVPE reactor under H_2 flow with a pressure of 10^4 Pa. The spectra are identical to those observed under UHV conditions. Again the typical '$c(4\times4)$' and '(2×4)' RAS spectra show up. The latter

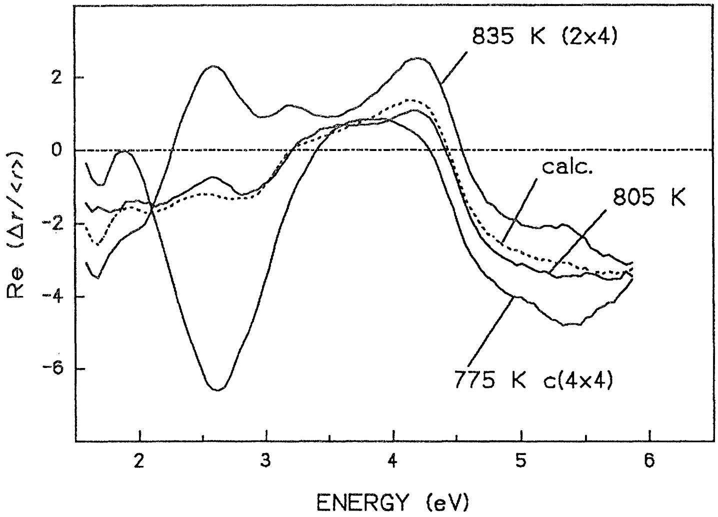

Figure 6. Three RAS spectra from figure 5 (solid lines). The dashed line is calculated as a linear combination of the 835 K spectrum (40 %) and the 775 K spectrum (60 %). It shows good agreement with the 805 K spectrum.

occurs at higher temperatures because arsenic is lost from the surface and thus favouring the less arsenic rich (2 × 4) surface.

The identity of RAS spectra from reconstructed surfaces under UHV conditions and gas phase conditions has led to the conclusion that under gas phase conditions the surfaces are also reconstructed. On the other hand, one has to note that RAS is not sensitive to long-range order like a diffraction experiment, but responds to susceptibility contributions from dimer bonds orientated along similar directions in the surface. Therefore, an anisotropic signal may arise even in cases where long range order is not very significant. Grazing X-ray diffraction experiments (GIXS) indicate such a situation in MOVPE growth (Kisker *et al.* 1992). Nevertheless we will associate the following the RAS spectra with the corresponding reconstructions.

The RAS spectra in figure 5 shows a continuous transition between the *c*(4 × 4) and (2 × 4) reconstructions. In RHEED or LEED either one with decreasing clarity or just diffuse background is visible. These intermediate RAS spectra can be described as a linear combination of the two spectra assigned to (4 × 4) and (2 × 4). This is demonstrated in figure 6 for the 805 K spectrum which is described approximately by 40 % contribution from a (4 × 4) and 60 % from a (2 × 4) RAS spectrum.

The loss of As from the surface can be prevented by adding arsenic containing precursors into the MOVPE gas flow. The effect of adding AsH_3 at a partial pressure of 70 Pa is demonstrated in figure 7. At a temperature of 825 K, where in the case of pure H_2 the (2 × 4) was dominating, now still the arsenic rich *c*(4 × 4) surface is present. Taking a different precursor, namely tertiarybutylarsine at a much lower partial pressure of 11 Pa, the loss of As is even more prevented (figure 8). Even at 1000 K still essentially the arsenic rich *c*(4 × 4) is dominating. The obvious conclusion, already expected from more indirect growth observations, is that tertiarybutylarsine is a much more efficient donator of arsenic than AsH_3. Such measurements can be utilized now to put the As stoichiometry of the surface into the right conditions for growth. From the standard growth parameter quoted in the literature for MOVPE growth of GaAs the optimum pregrowth conditions as close to a c(4 × 4) surface.

Figure 7

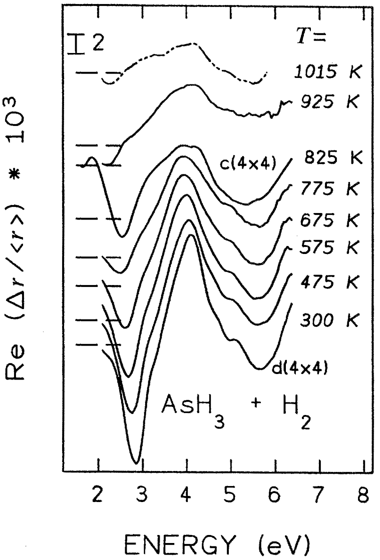

Figure 8

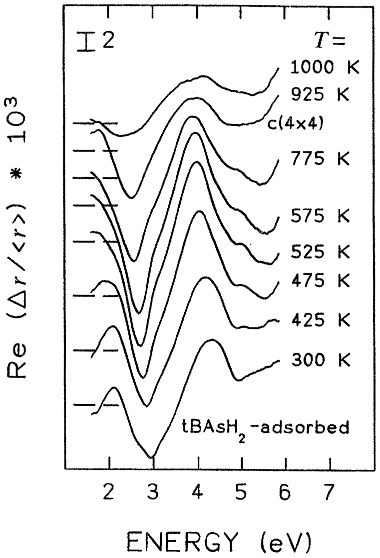

Figure 7. RAS spectra of GaAs (100) in an MOVPE reactor at different temperatures and with $p(H_2) = 10^4$ Pa, $p(AsH_3) = 70$ Pa.

Figure 8. RAS spectra of GaAs(100) in an MOVPE reactor at different temperatures and with $p(H_2) = 10^4$ Pa, $p(tBAsH_2) = 11$ Pa.

Starting growth of GaAs by adding trimethylgallium ($Ga(CH_3)_3$) the RAS spectra, shown up to now for arsenic stabilized conditions, change partly considerably. This is demonstrated in figure 9 for three different temperatures. The RAS spectra presented there for stationary growth conditions (solid lines) were taken with sampling times for each data point several times longer than the time needed to grow a monolayer of GaAs. The magnitude of change between the spectra before and during growth depends on the degree of As stabilization of the surface. At higher temperatures where at the AsH_3 partial pressure chosen (70 Pa) the surface before TMG addition is already close to a (2 × 4) essentially no difference exists between the surface before and after TMG addition. At lower temperatures where the surface is $c(4\times4)$ like the changes introduced upon TMG addition are quite strong. They appear especially at the spectral position where the As-dimer transitions are assumed to contribute to the polarizability (2.6 and 4.0 eV). These changes of course indicate that as a consequence of additional Ga on the surface a certain number of As-dimers directed along [110] as shown in figure 4 for the $c(4\times4)$ surface is now either destroyed or switches to the [110] direction as would be appropriate for the (2 × 4) surface.

The difference in the RAS signals between the pregrowth and stationary growth state spectra of course makes time resolved studies an interesting experiment. It is clear that the time variation (increase or decrease) of the signal depends on the choice of photon energy. With our equipment available at present, time resolved studies were only possible at a fixed wavelength. More elaborate designs which allow for a number of wavelength sampled simultaneously or with an optical multichannel analyser, possibly could perform time and spectral resolution simultaneously. However, since the phase shift of the photoelastic modulator is wavelength dependent (quartz) the data evaluation will be rather complex.

Figure 9

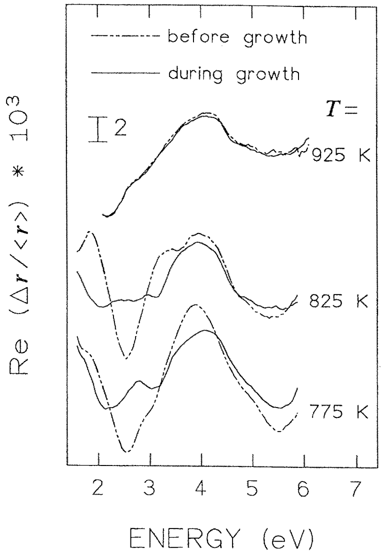

Figure 10

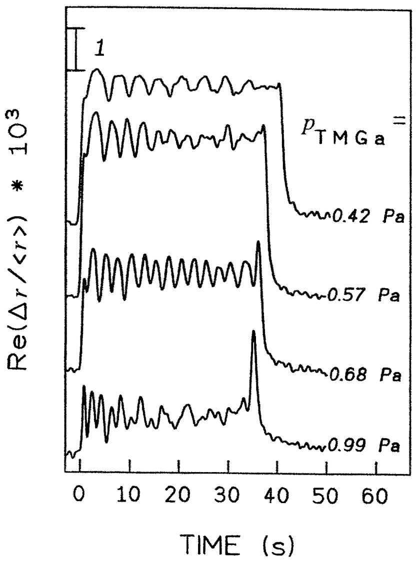

Figure 9. RAS spectra of GaAs(100) in an MOVPE reactor at three different temperatures and $p(H_2) = 10^4$ Pa, $p(AsH_3) = 70$ Pa without trimethylgallium (dashed line) and with $p(\mathrm{TMG}) = 0.42$ Pa (solid line).

Figure 10. RAS signal at a fixed photoenergy ($\hbar\omega = 2.6$ eV) on GaAs(100) and with $p(H_2) = 10^4$ Pa, $p(AsH_3) = 70$ Pa when starting growth by adding TMG at different partial pressures between $t = 0$ and $t = 35$–40 *s*.

In figure 10 the result of time resolved studies performed at 775 K and at a photon energy of 2.6 eV are shown for a number of different TMG partial pressures. The time $t = 0$ corresponds to the time where TMG has been switched on and is appearing at the substrate. The rise time as well the return time of the signal after shutting of the TMG (at $t = 35$–40 s) are experimentally limited here by the electronic time constant (lock-in). The magnitude of the rise at $t = 0$ corresponds to the difference between the two stationary RAS spectra at 775 K (figure 9), but taken now for a number of different TMG partial pressures. The most prominent features in figure 10 which appear after the first rise are of course the oscillations. Their frequencies increase with increasing TMG partial pressure. The time of one period corresponds to what is expected for the growth time of one monolayer of GaAs at these growth conditions. That these oscillations are really monolayer growth oscillations, is verified in figure 11. There the inverse time period multiplied with the monolayer thickness (0.283 nm) is plotted versus partial pressure of TMG (open squares). Included are also growth rate data determined from post-growth thickness measurements (filled squares). In this transport limited growth region the linear dependence on TMG partial pressure is expected (Heinecke *et al.* 1984). That both data-sets follow the same line proves that the oscillations correspond indeed to the growth of successive monolayers. While such oscillations have been observed already in MBE (Aspnes *et al.* 1987; Scholz *et al.* 1992) or in very low pressure epitaxial conditions (Samuelson *et al.* 1991), the observation in a standard MOVPE environment (10^4 Pa) has been only made very recently (Reindhardt *et al.* 1993*a*).

In summarizing RAS shows many features which enable the experimentator to draw similar conclusions about the growing surface as it can be done with RHEED in

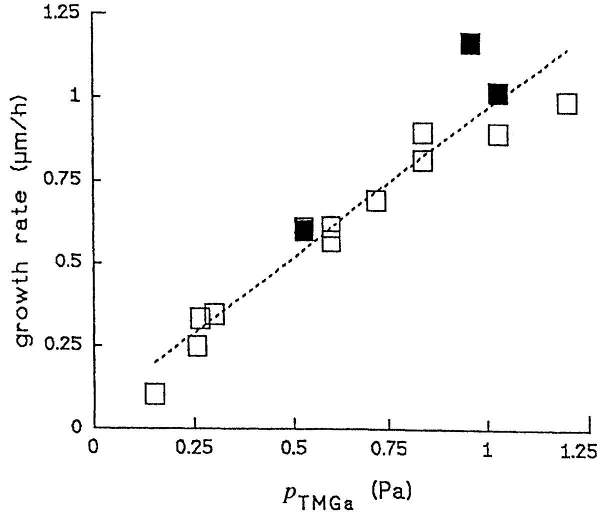

Figure 11. Growth rate determined from RAS signal oscillations (open squares) and from post-growth thickness measurements (filled squares); $T = 785\ K$, $p_{\text{tot}} = 100$ mbar.

MBE growth. Both RAS as well as RHEED allow to control pregrowth and growth conditions and moreover to determine the growth rate with monolayer resolution. The origin of these capabilities are of course different. In RHEED it is the morphology as shown in figure 1 and long range order (figure 4), while in RAS it is the more 'chemical' information originating from the surface bonds. The latter allows for a wider range of diagnostic applications among which for example substrate analysis at room temperature under ambient air should be mentioned (Reinhardt *et al.* 1993*b*). The result of the present study for MOVPE growth of GaAs show that the $c(4 \times 4)$ like surface is the standard pregrowth surface for GaAs and, moreover, that this surface is the necessary condition in order to observe monolayer growth oscillations.

3. Raman scattering study of MBE growth

As has become clear in the last section, control of MBE growth by RHEED gives mainly structural information on symmetry and morphology which combined with knowledge of surface physics can provide a quite successful control of growth. However, the more chemical information supplied by optical surface analysis is in certain cases, for example when interface reactions occur, of definite advantage. Such cases are for example constituted in the case of epitaxial growth of II–VI semiconductors on III–V-semiconductor substrates.

Raman scattering has been shown to be capable to detect and analyse vibrational properties at surfaces down to a monolayer level (Hünermann *et al.* 1991). The decrease of signal originating from the reduction of the scattering volume is compensated in these cases by carefully exploiting resonance conditions of the exciting laser light with electronic transition energies of the layer. In a few cases even submonolayer sensitivity has been achieved. The surface sensitivity of Raman scattering thereby derives from the fact that at a heterointerface different kinds of atoms are present. The vibrational properties then act as a fingerprint like feature and give information on which side of the interface the scattered light is originating. This is the specific feature which allows Raman scattering to discriminate surface

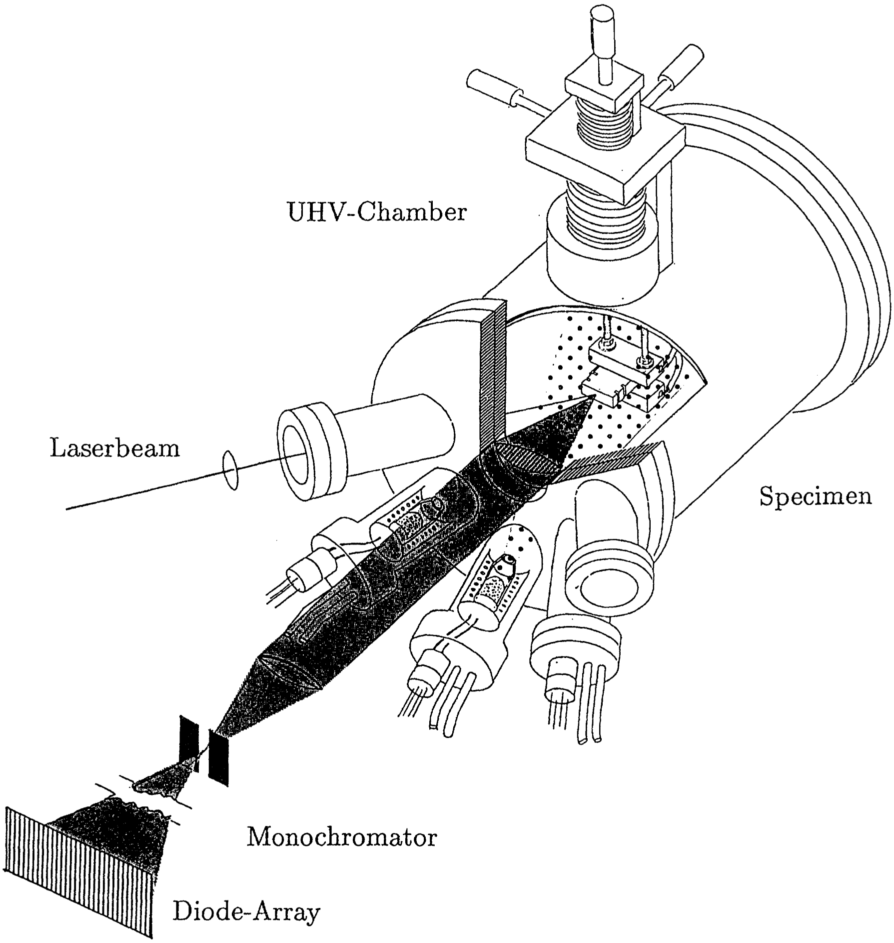

Figure 12. Schematic diagram of an MBE chamber with a front window designed for on line monitoring of semiconductor growth by Raman scattering. The schematic optical diagram with slit and diode array represents an optical multichannel Raman spectrometer with a subtractive double monochromator and a polychromator.

adsorbates or layers against the usually strong signals from the bulk. It seems therefore feasible to utilize the potential of Raman scattering also for *in situ* and online investigations of epitaxial growth.

To study the growth of heterointerfaces we have combined a MBE apparatus with an optical multichannel Raman spectrometer as outlined in figure 12 (Wagner *et al.* 1993). The MBE chamber is equipped with three Knudsen cells and with a number of optical windows which allow to focus the exciting laser light onto the growing surface. The scattered light itself is collected by a $f/4$ lens positioned at the front wall of the chamber and further away it is focused onto the entrance slit of the Raman spectrometer. The Raman spectrometers allows for taking a spectrum with a minimum time of 10 s. However, to achieve a reasonable signal to noise ratio the typical collecting time for a spectrum was around 30 s per spectrum. In addition, since the time variation of the Raman spectra on this timescale was usually weak, up to ten spectra were averaged afterwards.

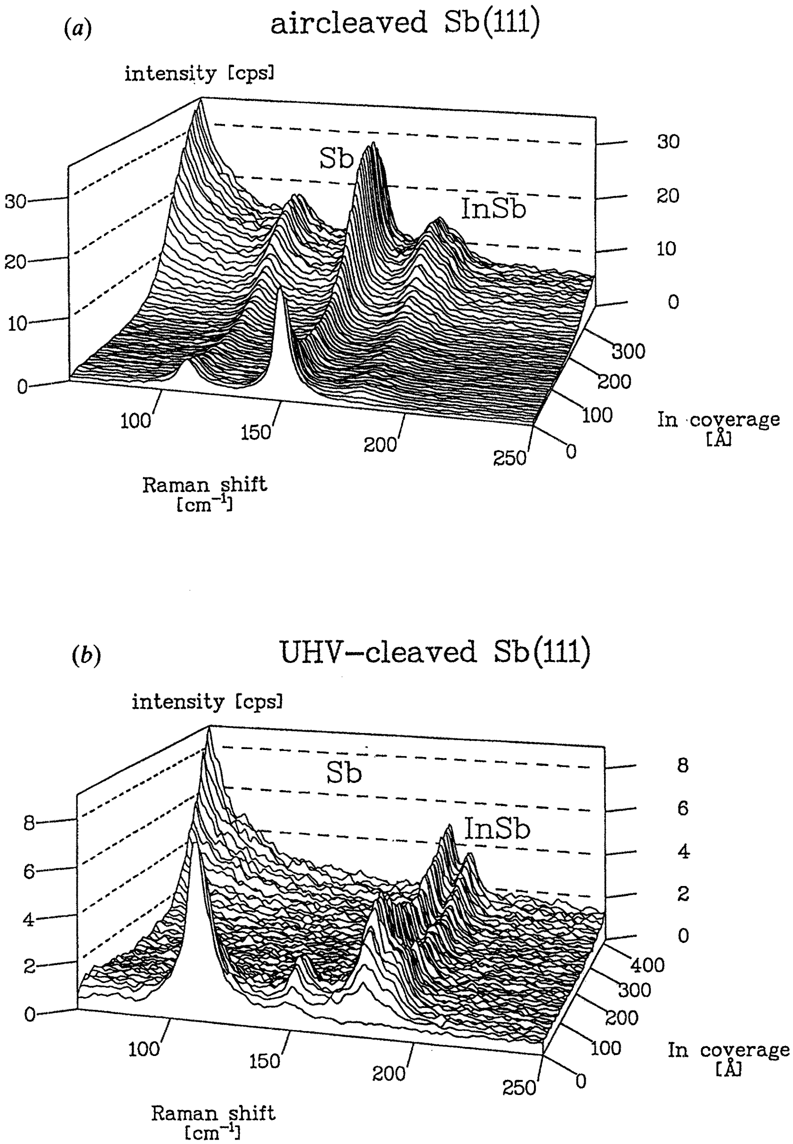

Figure 13. On line Raman spectra of InSb MBE growth on Sb(111) with one indium Knudsen cell. In (*a*) the Sb (111) surface was cleaved in air and annealed at 370 K. In (*b*) the Sb(111) surface was obtained by cleaving under UHV conditions. The indium coverage is the value deposited nominally on the surface (Wagner *et al.* 1993).

Two examples will be discussed. The first, the growth of InSb on Sb substrates, if of course not so much of technological interest, but has received considerable attention in the literature (Delrue *et al.* 1986). This is mainly because the growth method gives a simple possibility to grow a number of different III–V semiconducting compounds. Moreover, it serves the purpose to demonstrate here nicely the features of online Raman monitoring. The second example is concerned with the growth of CdTe on InSb, a heterosystem which is known to show strong interface reaction (Zahn *et al.* 1987).

Growth requires in this case just one single Knudsen cell which deposits In on the

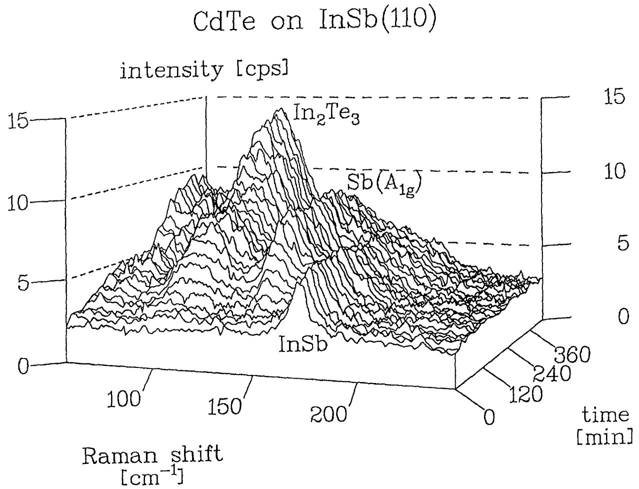

Figure 14. Coverage dependence of E_g-mode (113 cm^{-1}) of Sb from figure 13. The solid line represents the exponential absorption (Beers law) of the InSb top layer, while the dashed line takes into account multiple reflection effects within the layer.

Sb surface (Delrue *et al.* 1986). The In reacts already at room temperature with Sb and forms epitaxial InSb layers with (111) orientation on cleaved Sb(111) surfaces. At higher growth temperatures than room temperature the crystalline quality is slightly increased. Figure 13*a*, *b* shows results on the growth of InSb on two differently prepared Sb surfaces. In both cases the Sb(111) surfaces were obtained by cleavage. In figure 13*a* the substrate was cleaved in air and annealed in UHV at a temperature of 370 K, while in figure 13*b* the substrate was cleaved in UHV and no further treatment was performed. In both cases the Raman spectra from the pure substrate are the ones appearing in front of the three-dimensional plot, taken before In deposition starts. They show the typical Sb features with two peaks corresponding to the E_g (113 cm^{-1}) and the A_g (150 cm^{-1}) phonons of Sb. In both cases, with increasing indium deposition, structure in the 180–190 cm^{-1} spectral region occurs. This is the phonon structure due to the InSb zone centre ($k = 0$) optical phonons (TO: 180 cm^{-1}; LO: 191 cm^{-1}). The phonons are more clearly resolved in the UHV-cleaved case than in the aircleaved case. This indicates a smaller linewidth and a more perfect lattice structure for InSb grown on a UHV cleaved substrate.

The most significant difference between the two growth runs, however, is the intensity variation of the Sb phonon peaks with increasing In deposition. While in figure 13*a* the phonon peaks remain visible throughout the whole deposition process, in figure 13*b* they disappear after the deposition of approximately 10 nm of In. The latter behaviour is expected in the case of layer by layer growth. The scattered light originating from the substrate is absorbed through the growing InSb layer and similarly is the exciting laser intensity available at the substrate. This leads in first approximation to an exponential decay of the scattered light intensity. Such a dependence is indeed observed as shown in figure 14. From the known absorption constant of InSb it is then possible to determine the thickness of the growing InSb layer and consequently also the growth rate.

The different behaviour of the scattered light intensity in figure 13*a* on the other hand can only be explained if large parts of the substrate are covered only by a very thin InSb layer or not at all. It must be concluded that in the aircleaved case InSb

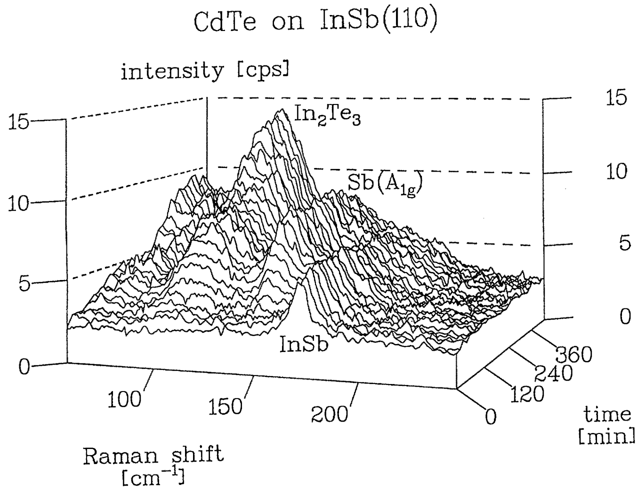

Figure 15. On line Raman spectra of MBE growth of CdTe (evaporated from solid CdTe) on InSb (110). Since the interface is highly reactive In_2Te_3 is formed and Sb liberated. No indication of CdTe can be found in the Raman spectra (after Zahn *et al.* 1987).

is mainly grown in islands. Raman scattering, therefore, is also quite capable to classify the growth morphology.

A further example showing the potential of Raman scattering is given in figure 15 with the deposition of CdTe from a single Knudsen cell onto InSb at 570 K. It is known that under these conditions strong reactions occur. Indeed the figure shows the appearance of phonon peaks which must be assigned to In_2Te_3 and the A_{1g} peak of Sb. This is in agreement with previously published data which explained this behaviour with the strong reaction of Te with In to form the thermodynamically most stable In_2Te_3 compound and thereby liberating Sb from the InSb (Zahn *et al.* 1987). This reaction is quite strong and therefore no CdTe is observed at all. Such interface reaction probably would be difficult to detect with RHEED since the growth of the III_2VI_3 compounds crystallizing in the zincblende defect structure on III–V substrates shows epitaxial behaviour.

4. Conclusions

Two optical techniques, reflectance anisotropy spectroscopy and Raman scattering, have been applied to epitaxial growth. They allow to obtain information on substrate quality, substrate pregrowth conditions, growth rate, interface structure and growth morphology. This information can be obtained on a time scale which allows in most cases real time analysis. It can therefore be stated that optical techniques are now ready to be utilized in monitoring of growth but other surface modifications as well. They have no restrictions as far as the environment is concerned and may be applied in ultrahigh vacuum as well as in high pressure applications. Comparing with RHEED, the 'standard' analysis tool in MBE, the optical techniques moreover provide additional information since they are not dependent on long-range order.

The contributions of my co-workers, D. Drews, A. Müller, K. Ploska, F. Reinhardt, K. C. Rose, V. Wagner, D. R. T. Zahn, to the results presented here is gratefully acknowledged. Financial support was obtained through the ESPRIT Basic Research Action 6878 'EASI' and a DAAD grant.

References

Aspnes, D. E. 1985 *J. Vac. Sci. Technol.* B3, 1498.

Aspnes, D. E., Bhat, R., Colas, E., Florez, L. T., Harbison, J. P., Kelly, M. K., Keramidas, V. G., Koza, M. A. & Studna, A. A. 1989 *Proc. SPIE* **1037**, 2.

Biegelsen, D. K., Bringans, R. D., Northrup, J. E. & Swartz, A. 1990 *Phys. Rev.*, B **41**, 5701.

Chang, Y.-C. & Aspnes, D. E. 1990 *J. Vac. Sci. Technol.* B **8**, 896.

Delrue, J. P., Sporken, R. & Caudano, R. 1986 *J. Vac. Sci. Technol.* A **4**, 754.

Heinecke, H., Veuhoff, E., Pütz, N., Heryen, M. & Balk, P. 1984 *J. electron. Mater.* **13**, 816.

Herrman, M. A. & Sitter, H. 1989 *Molecular beam epitaxy*. Berlin, Göttingen and Heidelberg: Springer.

Hünermann, M., Geurts, J. & Richter, W. 1991 *Phys. Rev. Lett.* **66**, 640.

Joyce, B. A., Dobson, P. J., Neave, J. H., Woodbridge, K., Zhang, J., Larsen, P. K. & Boelger, B. 1986 *Surf. Sci.* **186**, 423.

Kamiya, I., Aspnes, D. E., Florez, L. T. & Harbison, J. P. 1992 *Phys. Rev.* B **46**, 15894.

Kisker, D. W., Stephenson, G. B., Fuoss, P. H., Lamelas, F. J., Brennan, S. & Imperatori, P. 1992 *J. Cryst. growth* **124**, 1.

Koch, S. M., Acher, O., Omnes, F., Defour, M., Drevillon, B. & Razeghi, M. 1990 *J. appl. Phys.* **68**, 3364.

McGilp, J. F. 1990 *J. Phys.: Condens. Matter* **2**, 7985.

Razeghi, M. 1989 *The MOCVD challenge*. Bristol: Adam Hilger.

Reinhardt, F., Richter, W., Ploska, K., Kurpas, P. & Rose, K. 1993*a* *Appl. Phys. Lett.* (In the press.)

Reinhardt, F., Richter, W., Müller, A. B., Gutsche, D., Kurpus, P., Ploska, K., Rose, K. C. & Zorn, H. 1983*b* *J. Vac. Sci. Technol.* (In the press.)

Resch, U., Scholz, S. M., Rossow, U., Müller, A. B. & Richter, W. 1992 *Appl. Surf. Sci.* **93**, 605.

Samuelson, L., Deppert, K., Jeppesen, S., Jönsson, J., Paulsson, G. & Schmidt, P. 1991 *J. Crystal Growth* **107**, 68.

Scholz, S. M., Müller, A. B., Richter, W., Zahn, D. R. T., Westwood, D. I., Woolf, D. A. & Williams, R. H. 1992 *J. Vac. Sci. Technol.* B **10**, 1710.

Wagner, V., Drews, D., Emde, M. v. d., Esser, N., Zahn, D. R. T., Geurt, J. & Richter, W. 1993 *Appl. Phys. Lett.* (In the press.)

Weightman, P. 1991 *Phys. World* **4**, 39.

Zahn, D. R. T., Mackey, K. J., Williams, R. H., Münder, H., Geurts, J. & Richter, W. 1987 *Appl. Phys. Lett.* **50**, 742.

Discussion

J. F. McGilp (*Dublin University, Ireland*). After these two excellent talks about monolayer-sensitive optical techniques ('epioptic' techniques (McGilp 1990)), it may be helpful to place them in context by considering the type of measurement being looked for, and the materials systems of interest. The main developing areas are, in my view, real time growth monitoring in MOVPE systems, and general *in situ* characterization in all growth ambients, the latter being driven by interest in nanostructures and ULSI in general, and single wafer processing of silicon in particular.

As regards real-time growth monitoring, monolayer counting and alloy composition control have been demonstrated for III–V systems using various polarized linear reflectivity techniques (ellipsometry, reflection anisotropy spectroscopy – also called reflection difference spectroscopy, surface photoabsorption). It is likely that these techniques will also be helpful for II–VI and IV–IV materials systems where, in the latter case, real-time Si–Ge alloy composition control should be possible.

As regards more general *in situ* characterization, monolayer sensitivity has been demonstrated, additionally, using Raman spectroscopy, as Professor Richter mentioned, photoluminescence, as Professor Hasegawa also discusses, Fourier transform infrared spectroscopy, optical second harmonic generation, and surface X-ray diffraction, as Dr Norris discusses.

I would identify two areas of weakness at present. The first is in developing useful, predictive theories of the optical response of surface and interfaces, and the second is in developing monolayer counting techniques for growth on Si(001) surfaces, the main surface of the semiconductor electronics industry. The problem here is that, although the surface reconstruction has in-plane anisotropy, the two-domain structure of singular surfaces largely removes this anisotropy, making the use of polarized linear reflectivity techniques very difficult.

Additional reference

McGilp, J. F. 1990 *J. Phys.: Condens. Matter* **2**, 7985.